NJC

Accepted Manuscript

This is an *Accepted Manuscript*, which has been through the Royal Society of Chemistry peer review process and has been accepted for publication.

Accepted Manuscripts are published online shortly after acceptance, before technical editing, formatting and proof reading. Using this free service, authors can make their results available to the community, in citable form, before we publish the edited article. We will replace this *Accepted Manuscript* with the edited and formatted *Advance Article* as soon as it is available.

You can find more information about *Accepted Manuscripts* in the Information for Authors.

Please note that technical editing may introduce minor changes to the text and/or graphics, which may alter content. The journal's standard Terms & Conditions and the Ethical guidelines still apply. In no event shall the Royal Society of Chemistry be held responsible for any errors or omissions in this *Accepted Manuscript* or any consequences arising from the use of any information it contains.

ROYAL SOCIETY OF CHEMISTRY

www.rsc.org/njc

Table of Contents (TOC)

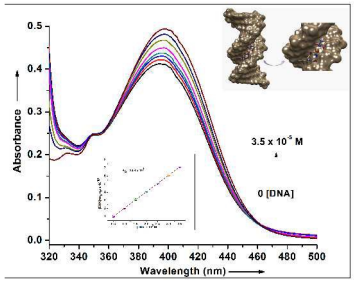

Interactions of Pt(Ura)(GL) with DNA

Physicochemical properties of the ternary complexes of Pt(II) with uracil and small peptide moieties: an experimental and computational study

Shilpi Mandal[a], Gunajyoti Das*[b] and Hassan Askari[a]

[a]*Centre of Advanced Study and Department of Chemistry, North-Eastern Hill University, Shillong-793022, Meghalaya, India.*
[b]*Department of Chemistry, Central Institute of Technology, Kokrajhar-783370, BTAD, Assam, India.*
**E-mail: guna_das@yahoo.co.in*

Abstract

A combined experimental and theoretical approach has been adopted to study the formation of mixed ligand peptide-nucleobase complexes of platinum(II), considering uracil as the primary ligand and dipeptides such as glycyl-*l*-valine, glycyl-*l*-leucine and *l*-alanyl-*l*-glutamine as secondary ligands. The ternary complexes prepared in both solid and aqueous phases, by following two synthetic procedures i.e. solvent-free mechanochemical and co-precipitation methods respectively, exhibit similar physicochemical and spectral properties providing evidences of metal-coordination through the N_3 and O_4 atoms of uracil as well as the NH_2 and CO_2^- functions of the dipeptide molecules. Using the biologically relevant right-handed α-helical conformers of the dipeptides, gas and aqueous phase quantum mechanical modeling studies are undertaken employing the B3LYP and B3PW91 methods in conjunction with the 6-31++G(d,p) and LANL2DZ basis sets to elucidate the roles of metal-coordination and solvation in influencing the structural, electronic and vibrational properties of the complexes. The Pt(II) ion is found to exist in its low-spin state in the complexes. Effects of explicit aqueous environment on the structural aspects of the complexes are also investigated. The B3LYP functional emerges to be more efficient in describing the vibrational spectroscopy of the studied systems as compared to the B3PW91 method. Absorption titration experiments followed by *in silico* docking and molecular mechanical studies reveal that the synthesized complexes are able to bind to DNA minor-groove, primarily through H-bonding interactions.

Introduction

Platinum complexes of nucleic acid bases, amino acid residues, as well as small peptide moieties hold great promise as model systems to understand the nature and significance of the interactions of metal ions with proteins and nucleic acid molecules, metal ion-provoked important cellular events like protein-nucleic acid interactions, and the effects this rarely occurring element produces in biological systems exposed to it.[1-5] Several low molecular weight amino acid sequences are endogenously produced in living systems that perform numerous key biological roles.[6] Dipeptides such glycyl-*l*-valine and *l*-alanyl-*l*-glutamine are known for their clinical and nutritional importance[7,8] The scientific, biological, and industrial significance of the study of peptide-metal ion interactions have been well documented in the past few years.[9-11] Uracil, one of the four nucleobases of ribonucleic acid which is generally believed to have been introduced to the prebiotic earth extraterrestrially by small solar system bodies,[12] has on several occasions been subjected to complex formation by a host of metal ions employing a number of experimental and theoretical techniques.[13-18] However, assessment of the literature reveals that the prospects of the solid-phase formation of mixed ligand complexes of Pt(II) ion with uracil and dipeptide moieties in a 1:1:1 molar ratio under solventless conditions; their DNA-binding aspects and affinities; and the efficiency of the commonly used density functional theory (DFT) based methodologies in predicting the physicochemical and spectral properties of such complexes have not been investigated yet.

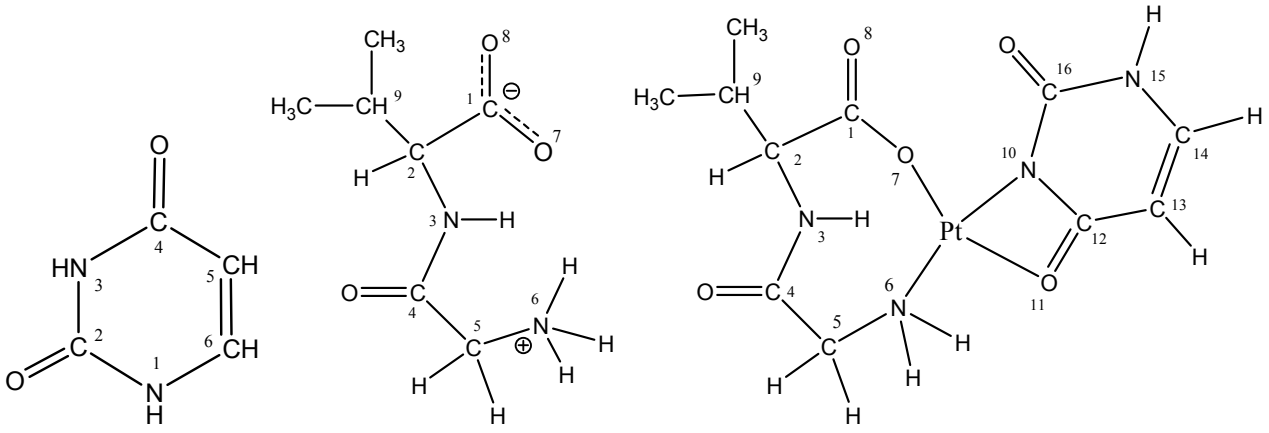

Fig.1 Uracil, zwitterion glycyl-*l*-valine and their complex with Pt(II)

This study reports the preparation of three Pt(II) mixed ligand complexes of uracil (Ura) as a primary ligand and dipeptides such as glycyl-*l*-valine (GV), glycyl-*l*-leucine (GL) and *l*-alanyl-*l*-glutamine (AG) (where the first amino acid residue corresponds to the amino-terminus of the dipeptides) as secondary ligands employing a solvent-free mechanochemical (hand-grinding) method.[19] The co-precipitation method is used to study the interaction motifs of the considered ligands with Pt(II) ion in aqueous environment as well. Characterization of the metal complexes are carried out using elemental analyses; molar conductance; TEM and SEM-EDAX; TG/DTA; infrared, electronic absorption and mass spectroscopy. Fig. 1 illustrates the molecular geometries of the zwitterion GV and its complex with Ura and Pt(II). Considering the most predominant conformers of the dipeptides, selected on the basis of a conformational analysis at B3PW91/6-31++G(d,p) level in aqueous phase, complementary geometries of the metallic complexes are modeled within the framework of density functional theory utilizing the B3LYP and B3PW91 methods in conjunction with 6-31++G(d,p) basis set (LANL2DZ for Pt(II) ion). The gaseous and aqueous phase interaction enthalpies and free energies (ΔH and ΔG respectively); theoretical IR and UV-vis spectra; HOMO-LUMO energy gaps; dipole moments; Wiberg bond indices as well as the partial atomic charges in the ligand molecules and their metallic complexes are calculated and evaluated. An explicit solvation model is also used for the Pt(Ura)(GV) complex, incorporating four discrete water molecules primarily around the peptide bond of the complex, this hydrated complex being denoted as ^{w}Pt(Ura)(GV). The DNA-binding motifs and binding-affinities of the synthesized complexes are studied by performing absorption titration experiments together with *in silico* docking and molecular mechanical studies. It is expected that evaluation of the metal-coordinating properties of uracil and small peptide moieties in both solid and aqueous phases as well as examination of the efficiencies of the B3LYP and B3PW91 methodologies in ascribing the electronic and spectral properties of metalated uracil and dipeptides may be useful from the methodological point of view. Information fetched from this study may also aid the pursuit of developing precise molecular mechanical force field parameters/libraries for biomacromolecular systems, besides benefiting the field of rational design of metalloproteins and novel DNA-binders.

Experimental and computational details

Materials used and synthesis of reaction products. Platinum(II) chloride (Loba Cheme), uracil (sigma-aldrich), the three dipeptides i.e. glycyl-*l*-valine, glycyl-*l*-leucine and *l*-alanyl-*l*-glutamine

(Himedia), calf thymus DNA (Himedia) and the other reagents used in the experiments were analytical reagent grade and used as supplied.

Synthesis in the solid-phase: The mixed ligand Pt(II) complexes of Ura and the dipeptides were prepared by following the solvent-free grinding method outlined already in our previous studies;[19] where the ligands and platinum(II) chloride, ground separately beforehand at room temperature for about 15 min in an agate mortar and pestle, were mixed in 1:1:1 (Pt(II):Ura:dipeptide) stoichiometry and ground again at room temperature for 60 min. The mixtures were heated in an air-thermostat at 80 ^{o}C for 36 h in order to accelerate the reactions. To ensure complete reaction the process of grinding, pulverization and heating was repeated several times. Ether was used to wash the final products, which were then finally dried under reduced pressure over anhydrous $CaCl_2$ in a desiccator. The progress of the reactions and purity of the products were monitored by TLC using silica gel G (yield: 87-92%).

Preparation in the solution-phase: Solution-phase preparations of the complexes were accomplished by the mixing of 50 mL aqueous solution of platinum(II) chloride (10 mmol; Millipore water; pH ~ 7) with 50 mL aqueous solutions of Ura and the dipeptides (10 mmol; Millipore water; pH ~ 7) in 1:1:1 ratio (Pt(II):Ura:dipeptide). The mixtures were then refluxed on water bath for 12 h. The precipitated complexes, appeared on standing and cooling the above solution, were filtered, washed with ether and dried under reduced pressure over anhydrous $CaCl_2$ in a desiccator. The products were further dried in electric oven at 50-70^{o}C (yield: 69-75%).

Instrumental details. The complexes were analyzed for C, H, and N contents on PerkinElmer 2400 Series II CHN-OS Analyser. The molar conductance values were measured in DMSO (10^{-3} M) solution using a coronation digital conductivity meter (cell constant = 1.0 cm^{-1}). Infrared spectra of all the reaction species were recorded in KBr discs on a BOMEM DA-8 FTIR spectrophotometer at 4000-400 cm^{-1}. The electronic absorption spectra of the complexes were also recorded in DMSO solution (10^{-5} M) on a Perkin Elmer lambda 25 UV/Vis spectrometer. The dehydration level of DMSO was 99%. The thermogravimetric (TG) and differential thermal analysis (DTA) measurements were carried out for the reaction products obtained by the grinding method in controlled nitrogen atmosphere on a Perkin-Elmer STA 6000 Simultaneous Thermal Analyser at temperature ranging from 40 to 800 °C at heating rate 20 °C/min. The EDAX-SEM micrographs for the Pt(Ura)(GV) complex were obtained in a Jeol, JSM-6360 LV apparatus, using an accelerating

voltage between 15–20 kV at different magnifications. TEM images were obtained on a JEOL-JEM-2100CX electron microscope operated at 200 kV without adding any contrast agent. Melting points of all the reaction species were also determined on an IkonTM Instrument.

Evaluation of DNA binding properties. Taking the case of the Pt(Ura)(GL) complex as a example, evaluation of the DNA-binding properties of the synthesized complexes was done with the aid of absorption titration experiments where homogeneous calf thymus DNA (CT-DNA) solutions of varying concentrations (0-35 μM) dissolved in a tris-HCl buffer (pH 7) were added to the aqueous solution of the test complex (10 μM dissolved in Millipore water). The concentration of CT-DNA was determined by UV absorbance at 260 nm. The protein-free nature of the DNA was confirmed by the fact that the solutions of CT-DNA gave a ratio of UV absorption at 260 and 280 nm A_{260}/A_{280} of ~ 1.8–1.9 (Fig. S1 of the SI).[20] The intrinsic binding constant (K_b) value for the interactions of the complex with CT-DNA was determined from the spectroscopic titration data using the following equation:[21]

$$[DNA]/ (\varepsilon_a - \varepsilon_f) = [DNA]/ (\varepsilon_b - \varepsilon_f) + 1/ K_b(\varepsilon_b - \varepsilon_f) \quad \text{..... (I)}$$

The "apparent" extinction coefficient (ε_a) was obtained by calculating $A_{obsd}/[DNA]$, while the terms ε_f and ε_b correspond to the extinction coefficients of the unbound (free) and fully bound complex respectively. The K_b value of the complex was obtained from the ratio of the slope to the intercept, $1/(\varepsilon_a - \varepsilon_f)$ and $1/K_b(\varepsilon_b - \varepsilon_f)$ respectively, given by the plot of $[DNA]/(\varepsilon_a - \varepsilon_f)$ versus [DNA]. The measurements were made at room temperature using the aforesaid UV-vis spectrometer.

Computational methods. The molecular structures of all the various ligands, their complexes with Pt(II), and the other reaction species involved in the equation (II) & (III) (given below) were subjected to full geometry optimization and vibrational frequency calculations employing the B3LYP[22,23] and B3PW91[24] methodologies in combination with the 6-31++G(d,p)[25,26] and LANL2DZ[27,28] basis sets of Gaussian 09 (Rev. C.01) program.[29] The solvated zwitterion AG molecule was subjected to a conformational analysis at the B3PW91/6-31++G(d,p) level about the dihedral angles α_1, α_2 and α_3 by rotating from 0° to 360° at 20° intervals. The minima identified on the conformational potential energy surfaces related to α_1, α_2 and α_3 were then fully optimized followed by frequency analyses in aqueous phase at B3PW91/6-31++G(d,p). The computations were

performed in a vacuum and aqueous phase using a polarizable continuum model (PCM).[30] The dipeptide structures were considered as non-ionic entities in the gas phase while as zwitterions in the aqueous phase. All the optimized geometries were confirmed as true minima by the absence of any imaginary frequency value in their vibrational frequency calculations. The accuracy of the theoretical calculations, performed using the B3LYP and B3PW91 functionals in conjunction with the 6-31++G(d,p) and LANL2DZ basis sets, in predicting the physicochemical features of a host of platinum complexes has been justified in the literature.[31,32] Furthermore, the efficacy of the B3LYP functional in complementing the experimental vibrational modes was noted in our earlier investigations.[33] Efficiency of the self-consistent reaction field (SCRF) procedure[34] as well as the usefulness of diffuse and polarization functions have also been well documented.[35] Zero-point energy (ZPE) corrections were applied to the total energies of all the reaction species using a correction factor 0.97.[19] The theoretically predicted vibrational frequencies of the ligands and their complexes were scaled using appropriate correction factors;[19] 0.977 for the modes below 1,800 cm^{-1} and 0.955 for those above 1,800 cm^{-1}. The values of ΔH and ΔG in the gaseous and aqueous phases were calculated using the equations given below:

$$\text{Dipeptide}_{zwitterion} + \text{Uracil} + PtCl_2 \xrightarrow[\text{phase}]{\text{Solvent}} \text{Pt(Ura)(Dipeptide)} + 2HCl \quad \text{..... (II)}$$

$$\text{Dipeptide}_{nonionic} + \text{Uracil} + PtCl_2 \xrightarrow[\text{phase}]{\text{Gaseous}} \text{Pt(Ura)(Dipeptide)} + 2HCl \quad \text{..... (III)}$$

Thus, ΔH or $\Delta G = [Et_{pdts}] - [Et_{rcts}]$,

where, Et_{pdts} and Et_{rcts} are the sum of the total electronic or free energies (ZPE corrected) of the products and reactants respectively. Single-point calculations were performed using time dependent density functional theory (TD-DFT)[33,36] in gaseous and aqueous phases at the B3PW91/6-31++G(d,p) level to obtain the theoretical λ_{max} values. Molecular docking studies were performed by HEX 8.0.0 software[37] using the optimized solvated geometries of the complexes and the classical $d(CGCGAATTCGCG)_2$ B-DNA sequence created by Avogadro 1.1.1.[38] Visualization of the high scoring docked poses were done by UCSF Chimera molecular graphics program.[39]

Table 1 Physical, conductivity and analytical data of the synthesized complexes. The calculated values of elemental analysis are given in parentheses; values in square bracket are from solvent phase products.

Compound	Formula	Colour	F. W. (gm/mol)	M. Pt. (C^o)	Λ_M $\Omega^{-1}cm^2mol^{-1}$ (in DMSO)	Found (calc.) (%)			Yield (%)
						C	H	N	
Pt(Ura)(GV)	$C_{11}H_{16}N_4O_5Pt$	Orange Powder	479.356	220-230	5.7	27.51 (27.56) [27.52]	3.36 (3.36) [3.29]	11.57 (11.69) [11.67]	89 [72]
Pt(Ura)(GL)	$C_{12}H_{18}N_4O_5Pt$	Orange Powder	493.381	225-235	6.2	29.19 (29.21) [29.36]	3.60 (3.68) [3.65]	11.19 (11.36) [11.34]	92 [75]
Pt(Ura)(AG)	$C_{12}H_{17}N_5O_6Pt$	Orange Powder	522.380	250-255	5.9	27.56 (27.59) [27.58]	4.30 (4.28) [4.28]	13.49 (13.41) [13.39]	87 [69]

F.W. = Formula weight

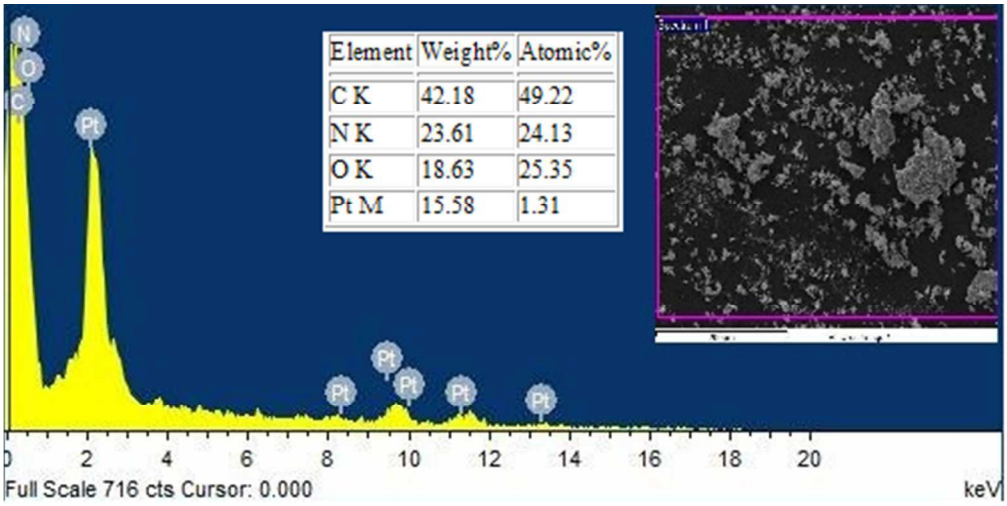

Fig. 2 EDAX spectrum of the Pt(Ura)(GV) complex

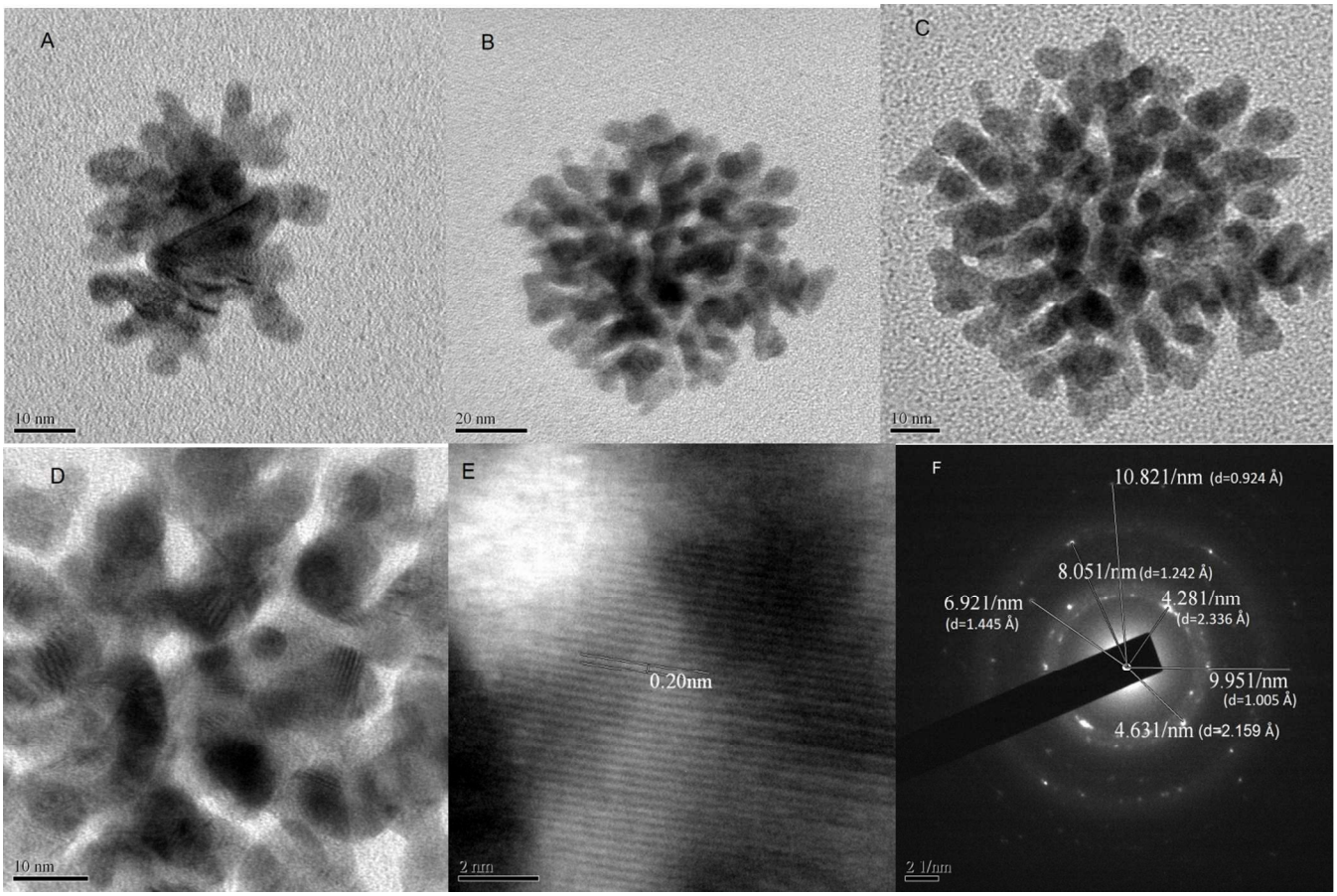

Fig. 3 TEM images of the Pt(Ura)(GV) complex prepared in solid state

Results and discussion

Physical, thermal and mass spectral properties. The physical, molar conductivity and analytical data of all the representative reaction species involved in the grinding and co-precipitation methods are assembled in Table 1. It is evident from these data that the colorations of the complexes obtained from both the solid-state grinding and the co-precipitation methods are same. The conductivity measurements of the complexes made in DMSO suggest that they are neutral and non-electrolytic in nature.[33] The results of the CHN-OS elemental analyses and the proposed formula of the synthesized complexes are found to compare well with their expected stoichiometries. The energy-dispersive X-ray analysis (EDAX), scanning electron microscopy (SEM) and transmission electron microscopy (TEM) images of the Pt(Ura)(GV) complex prepared in solid state are portrayed in Fig. 2 and 3. The SEM-EDAX image provides useful insights regarding the presence of platinum, chemical composition, purity, surface morphology and particle size of the complex under investigation. TEM images show that the particles are agglomerated and fall within a range of 6-10 nm in size. The HRTEM image shows the well-spaced lattice fringe indicating high crystalline quality of the complex with minimal dislocations and defects, whereas the SAED image bears information about its polycrystalline nature. The thermal properties of the complexes prepared by following the solid-phase grinding method have been examined using thermogravimetric (TG) and differential thermal analysis (DTA). Table 2 contains the maximum temperature values of decomposition along with corresponding weight loss values while the TG/DTA curves for all the complexes are reported in the Fig. S2. The TGA curves indicate that the metal complexes are thermally stable up to about 203-215 °C above which, *i.e.* between 203-797 °C, the actual mass loss steps begin and most of the organic parts of the metal complexes are lost during this period. This sharp decomposition period brings about 63-68% weight loss of the complexes leading to the formation of the residual products. The DTA curves of the metal complexes also show similar behavior that corresponds to the TGA curves. The small endothermic peaks at the range of 227-251 °C can be attributed to melting of the complexes. Mass spectra of the solid state products recorded at room temperature (Fig. S3) were used to compare the stoichiometric compositions of the ternary complexes. The molecular ion peaks for the Pt(Ura)(GV), Pt(Ura)(AG) and Pt(Ura)(GL) complexes observed at 479, 522 and 493 *m/z* respectively, are in good agreement with the analytical results.

Table 2 Summary of the TG/DTA analyses of the reaction products obtained by following the grinding method

Compounds	Decomposition range (^{o}C)	Peak temperature (^{o}C)	Percentage weight loss (%)	Product expected	Residue state/colour	Mass changes Calc. (found)
Pt(Ura)(GV)	215-790	227	63	Pt	Black Powder	2.69 (2.43)
Pt(Ura)(GL)	206-795	232	65	Pt	Black powder	2.30 (2.03)
Pt(Ura)(AG)	203-797	251	68	Pt	Black Powder	2.64 (2.25)

Conformation of the dipeptides. The conformational preferences of a particular dipeptide molecule about its Ramachandran dihedrals[40,41] (ψ and ϕ; shown in Fig. 1) have been well documented in the literature.[42,43] It is known that the $C7_{eq}$ (ψ= 90.1° and ϕ= -86.3°) and C5 (ψ= 143.8° and ϕ= -156.4°) conformers of the alanine dipeptide (AD) exist as the dominant entities in the gaseous and non-polar solvent phases,[42] whereas in a polar solvent the conformers C5, α_R (ψ= -32.1° and ϕ= -70.5°) and β (ψ= 142.1° and ϕ= -64.0°) emerge as the most predominant species with a relative thermodynamic stability order of C5 > α_R > β. However, since there is no existing experimental evidence of C5 as being the most stable conformer of a given dipeptide in the aqueous phase,[42] we opt to design the mixed ligand complexes using the biologically relevant right-handed alpha-helical conformers of the three dipeptides i.e. the α_R conformers of GV, GL and AG. In case of AG, the conformational propensities of the side-chain moiety of the glutamine residue has also been examined by carrying out a conformational analysis at B3PW91/6-31++G(d,p) level in aqueous phase. Fig. S4 illustrates the cross-section of the potential energy surfaces corresponding to the dihedrals α_1, α_2 and α_3 of the zwitterion *l*-alanyl-*l*-glutamine molecule while Fig. S5 portrays the B3PW91/6-31++G(d,p) level optimized structures and energies of the seven possible conformers corresponding to the aforementioned dihedral angles. The most stable AG6 conformer has been used to model the complex of *l*-alanyl-*l*-glutamine with Pt(II) and Ura. The gas and aqueous phase ZPVE corrected values (scaled with 0.97) of total electronic energies (E_c) and Gibbs free energies (G_c) of the ligands and their metal complexes at B3PW91 and B3LYP levels are presented in Table S1.

Table 3 Calculated interaction enthalpies ΔH (kcal/mol) and Gibbs energies ΔG (kcal/mol); dipole moments (μ; in Debye) and HOMO-LUMO energy gaps (E_{HL}; in eV) of the ligands and the complexes at B3PW91 level in gas and aqueous phases (listed in parentheses are the gas phase values)

Systems	ΔH	ΔG	ΔH^a	ΔG^a	μ	E_{HL}
Ura					6.276 (4.627)	5.625 (5.639)
GV					15.294 (7.120)	5.831 (6.251)
Pt(Ura)(GV)	-29.29 (-26.45)	-27.54 (-24.95)	-23.0 9 (-21.01)	-21.45 (-19.70)	11.822 (6.968)	4.672 (4.601)
Pt(Ura)(GV)[b]	23.75	23.98				
GL					15.051 (6.916)	5.849 (6.262)
Pt(Ura)(GL)	-26.71 (-25.35)	-24.84 (-23.56)	-20.30 (-19.78)	-19.69 (-18.06)	11.787 (6.933)	4.656 (4.604)
AG					20.634 (9.917)	5.727 (6.172)
Pt(Ura)(AG)	-27.39 (-27.03)	-26.00 (-25.14)	-21.70 (-20.23)	-20.39 (-19.52)	17.936 (12.465)	4.656 (4.274)

[a] Calculated using B3LYP; [b]Triplet

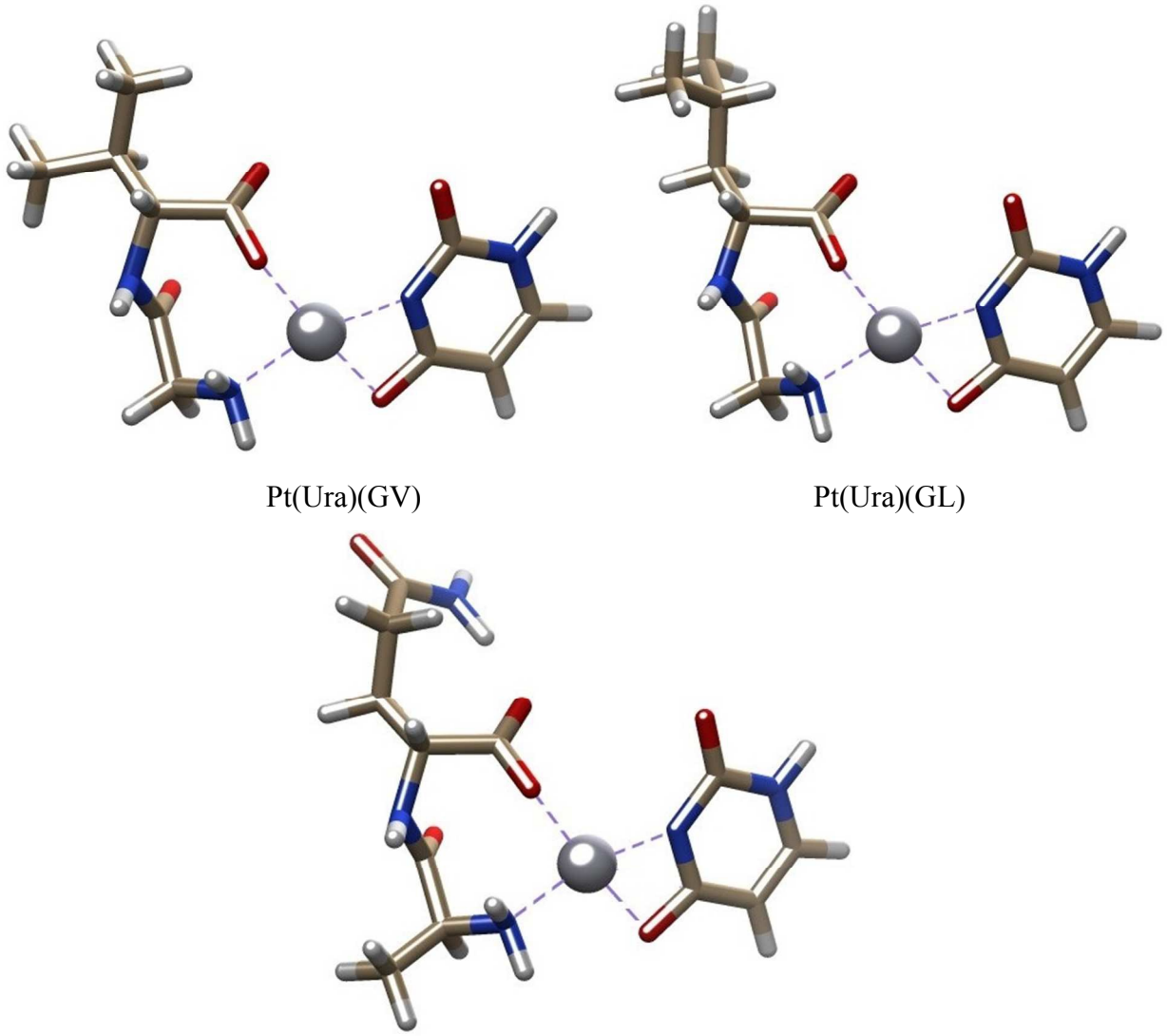

Fig. 4 B3PW91 level optimized geometries of the ternary complexes of Pt(II) in aqueous phase

Geometry and molecular properties. Portrayed in Fig.4 are the aqueous phase optimized geometries of the mixed ligand complexes of Pt(II) with uracil and the three dipeptide molecules calculated using B3PW91 functional in combination with 6-31++G(d,p) and LANL2DZ basis sets. These neutral and low-spin ternary complexes of Pt(II) are predicted to assume square planar geometries at their central metal cores by both the B3PW91 and B3LYP levels, which are consistent with the results of previous studies reported elsewhere in the literature.[44] Table 3 presents the calculated data on the interaction enthalpies and free energies, dipole moments and HOMO-LUMO

energy gaps of the ligands and their metallic complexes in the gaseous and aqueous phases. The thermodynamic stability of the complexes are reflected by their negative values of interaction enthalpies (-26.71 to -29.29 kcal/mol in aqueous phase and -25.35 to -27.03 kcal/mol in gas phase) and free energies (-24.84 to -27.54 kcal/mol in aqueous phase and -23.56 to -25.14 kcal/mol in gas phase), as calculated at the B3PW91 level. The trends of the interaction energies of the complexes (ΔH and ΔG values) obtained by using the B3LYP functional compare well with the ones furnished at B3PW91 level, though the B3LYP values are somewhat smaller as compared to those furnished at B3PW91 level. On other hand, the aqueous phase ΔH and ΔG values of the Pt(Ura)(GV)^b complex, 23.75 and 23.98 kcal/mol respectively, clearly show that the Pt(II) complexes of uracil and the dipeptides exist in their low-spin states. The theoretically obtained values of the total dipole moments of the reaction species suggest that the three complexes consistently possess smaller values of μ (11.787 D to 17.936 D in aqueous phase and 6.933 D to 12.465 D in gas phase) as compared to the corresponding free dipeptide molecules (15.051 D to 20.634 D in aqueous phase and 6.916 D to 9.917 D in gas phase). The lowering of μ values in case of the complexes can be due to loss of the dipolar structure (zwitterionic form) of the peptide moieties after complex formation. In the absence of any experimental data on the dipole moments regarding the type of complexes considered in this study, these theoretically predicted gas and aqueous phase values may serve as preliminary guideline for future experimentalist. Table 3 also represents the gas and aqueous phase data on the energy gaps between the highest occupied molecular orbital (HOMO) and lowest unoccupied molecular orbital (LUMO) energies. The important role played by HOMO and LUMO in governing chemical reactions was first noted by Fukui.[45] The predicted energy gaps of the ligands and their metal complexes are 4.656-5.849 eV in aqueous phase and 4.601-6.262 eV in gas phase. In case of the metal complexes, the furnished results suggest that the gas phase HOMO-LUMO energy gaps increase in the presence of a solvent with high dielectric constant. The decrease in the energy gaps of the dipeptides in aqueous phase compared to those in the gas phase can be attributed to the structural transformation from the neutral in vacuum to their zwitterionic form in the aqueous environment. The partial atomic charges of the ligands and the complexes predicted employing Natural Bond Orbitals (NBO) analyses at B3PW91 level in aqueous phase are collected in Table S2. The NPA charges reveal the partial atomic charge changes in the studied ligands as a result of metal coordination.

Experimental and theoretical vibrational assignments. The experimentally obtained FTIR spectra of the ligands (i.e. the dipeptides and uracil) and their mixed ligand Pt(II) complexes prepared by following the grinding and solvent phase methods are reported in the Fig. S6, while some of the structurally significant FTIR assignments are listed in Table S3. Comparison of the infrared assignments of the free zwitterion dipeptides (GV, GL, AG) with those of the complexes confirms the absence of any unreacted dipeptide molecules after the grinding or solvent phase procedures. As evident from Table S3, the appearance of $\nu(N_3\text{-}H)$, $\nu(C_4{=}O)$ and $\nu(C_4\text{-}N_3)$ vibrational modes of the amide moieties of the dipeptides and their mixed ligand Pt(II) complexes in the ranges of 3428-3449 cm^{-1}, 1687-1718 cm^{-1} and 1228-1237 cm^{-1} respectively in both solid and solvent phases suggests that the dipeptides do not interact with Pt(II) ions *via* their CONH groups.[43,46] On other hand, the asymmetric and symmetric ν(N-H) stretching modes of the three dipeptides (observed at 3251-3230 and 3110-3067 cm^{-1} respectively) are blue-shifted (3259-3232 and 3176-3116 cm^{-1} respectively) in their metal complexes. This indicates the deprotonation of the NH_3^+ moieties of the free dipeptides and subsequent binding to the Pt(II) ions through the amino nitrogen atoms.[33,43,47] Indication of metal coordination through the $–NH_2$ functions of the dipeptides is also provided by the fact that the $\nu(C_5\text{-}N_6)$ stretching values of the dipeptides (observed at 1102-1132 cm^{-1}) are red-shifted in the spectra of their metal complexes (1093-1127 cm^{-1}). The appearance of new strong bands in the range of 473-480 cm^{-1} in all the three metal complexes,[33,47] which can be assigned to asymmetric ν(M-N) stretching frequencies,[48] also confirms that the amino nitrogen atoms of the dipeptides are involved in metal coordination. Additionally, it is worth mentioning that the two coordinating $–NH_2$ groups are positioned *trans* to each other in the complexes since the symmetric ν(M-N) stretching mode of the N-M-N group (M= Pt(II)) which usually appears around 400-450 cm^{-1} is IR inactive.[43,48] Concerning the experimental infrared spectral data on the carboxylate groups of the dipeptides and their metal complexes, the $\nu_{as}(COO^-)$ modes of the dipeptides appearing at 1603-1626 cm^{-1} are found to shift toward the higher wave numbers of the frequency scale (up to 1667 cm^{-1}), whereas the $\nu_s(COO^-)$ stretches (observed at 1406-1454 cm^{-1}) shift to the lower-side in the complexes (1400-1419 cm^{-1}). These observations indicate that the dipeptides bind to the metal ions *via* their carboxylate functions.[33,43,47] Table S3 also gathers the differences (Δδ values) between the $\nu_{as}(COO^-)$ and $\nu_s(COO^-)$ stretches for the dipeptides and the metal complexes which are indicative of the M-O bond strengths and provide evidence that the COO^- groups bind to the metal ions in a monodentate fashion.[43,47] The Δδ values of the metal complexes ranging from 227 to 249 cm^{-1} indicate that the M-

O bonds possess significant covalent characters.[33,43,47] The new bands at 527-546 cm^{-1} in all the three metal complexes, which can be assigned to ν(M-O) stretching frequencies,[47] also confirm that the dipeptides interact with Pt(II) ions *via* their carboxylate groups. Thus, as observed for other metal-dipeptides complexes,[43,49] the experimental infrared spectra of this study furnish noticeable signatures indicating that the dipeptides bind to Pt(II) ions through their amino and carboxylate groups in both the solid and aqueous phases. The infrared spectrum of the free uracil molecule exhibits characteristic peaks at 3447, 3413, 1735 and 1765 cm^{-1} which could be assigned to $\nu(N_{15}$-H), $\nu(N_{10}$-H), $\nu(C_{12}$=O) and $\nu(C_{16}$=O) stretching modes respectively.[50] In case of the complexes, the $\nu(N_{10}$-H) modes are found to disappear; the carbonyl frequencies of the C_{12}=O groups are appreciably lowered; while other frequencies remain more or less unaltered.[51] These observations typify complex formation through the N_{10} and O_{11}-atoms of uracil.

The theoretical vibrational spectra of the dipeptides, uracil and their Pt(II) complexes were calculated using B3PW91 and B3LYP methods in combination with the 6-31++G(d,p) and LANL2DZ sets in the gaseous and aqueous phases. The theoretical harmonic frequencies are usually larger than their corresponding experimental values[52] and such discrepancies have been attributed to the neglect of anharmonicity effects in theoretical treatments, incomplete incorporation of electron correlation and the use of finite basis sets. Even then, the calculated vibrational modes of this study bear valuable information contributing to the understanding of the influence of metal binding and solvation effects on the structural and molecular properties of the ligands and the complexes. It has also been recognized that B3LYP level performs better in predicting the vibrational frequencies compared to MP2 level.[53] Collected in Table S3 are some of the structurally important frequency values of the representative reaction species calculated in both gas and aqueous phases. The theoretically predicted frequency-shifts of the ν_{as}(N-H), ν_{s}(N-H), $\nu_{as}(COO^{-})$ and $\nu_{s}(COO^{-})$ modes of the dipeptides as a result of metal coordination are found to corroborate well with the experimentally observed values. The calculated values of the ν(M-O) and ν(M-N) modes are also in good agreement with the experimentally observed ones. On other hand, the aqueous phase frequencies of the polar exposed bonds of the dipeptides and their complexes, namely N_3-H and C_4=O, are always lower as compared to their respective gas phase values and such lowering can be attributed to elongation of these bonds in the aqueous phase (see latter). Similarly, increase in the aqueous phase frequency values of $\nu(C_4$-$N_3)$ modes can be due to shortening of the C_4-N_3 bonds in the aqueous environment. Of the two methods, i.e. B3PW91 and B3LYP, it is the popularly used B3LYP functional which

seems to perform better in reproducing the experimental vibrational frequencies of the studied systems.

Table 4 Experimental and calculated absorption maxima (λ_{max}; in nm) of the synthesized complexes

Systems	Experimental λ_{max} in aqueous phase		Calculated λ_{max} at TD-B3PW91	
			Gas Phase	Aqueous Phase
	Solid state	Co-precipitation	Wave length	Wave length
Pt(Ura)(GV)	226, 299, 344, 423	219, 287, 484	384.63	405.84
Pt(Ura)(AG)	230, 295, 347, 424	217, 275, 464	383.35	470.55
Pt(Ura)(GL)	230, 310, 403	295, 360, 429	392.30	408.38

Electronic absorption properties. The optical properties of the ternary complexes of Pt(II), synthesized in both solid and aqueous phases, were studied using electronic absorption spectroscopy. Table 4 gathers the observed and calculated λ_{max} values of the complexes while their experimental and theoretical absorption spectra (calculated at TD-B3PW91 level) are stored in Fig. S7 & S8 respectively. The experimental UV-vis spectra of the complexes show intense absorption bands in the region 217-360 nm which are assigned to ligand-centered transitions. The additional less intense peaks at 403-484 nm can be attributed to LMCT transitions affirming the formation of the Pt(II)-peptide-nucleobase complexes with square planar type geometries at their metal cores.[44] The gas and aqueous phase theoretical electronic absorption spectra of the complexes furnish characteristic λ_{max} values around 383-392 nm in gas phase and 405-470 nm in aqueous phase; which are in good accord with the experimental observations.

Influence of complex formation and solvation on structural aspects. Atomic level structural information obtained from quantum chemical calculations regarding the effects of solvation and influence of metal coordination on the geometrical parameters linked to the backbone structural features of the dipeptides are crucial for the purpose of supporting or refuting the existing theories devoted to protein structure prediction. Some of the structurally significant bond length, bond angle and dihedral angle values of the dipeptides and the complexes calculated at B3PW91 level in gas and

aqueous phases are presented in Table S4. It is evident that out of the five bonds, namely C_2–N_3, N_3-H, C_4–N_3, C_4=O and C_4–C_5, considered to monitor the amide plane geometry of the dipeptides and the complexes, three of them i.e. C_2–N_3, C_4–N_3, and C_4–C_5 bonds of the complexes show maximum deviations up to 0.01 Å in aqueous phase (0.023 Å in gas phase) from those of the free ligand molecules. These changes indicate that the geometry about the amide plane of a given dipeptides is affected due to metal coordination. Considerable changes in the bond length values are also evident in the cases of C_1–C_2, C_5-N_6, C_1-O_7 and C_1-O_8 of the complexes, where the bond length values deviate up to a maximum of 0.035 Å in aqueous phase and 0.022 Å in gas phase. Furthermore, in the aqueous phase the C_4=O bonds of the dipeptides and complexes are elongated up to 0.011 Å while the C_4–N_3 bonds are shortened by a maximum value of 0.014 Å from their corresponding gas phase values. These variations are found to leave noticeable signatures in the theoretical IR spectra of the dipeptides and their complexes as already discussed in a previous section of this paper. Table S4 also represents the gas and aqueous phase values of the bond length for the M-O and M-N bonds of the metal complexes along with their Wiberg bond indices.[54] The Wiberg bond indices are helpful in estimating the bond order and, hence, the bond strength between two chemically bonded atoms. These data suggest that the Pt-O_7 bonds arising from the interactions of the dipeptides with the Pt(II) ions are stronger (in aqueous phase the bond lengths are in the range of 2.051-2.053 Å and bond indices span a scale of 0.375-0.390) as compared to the Pt-O_{11} bonds arising from uracil (in aqueous phase the bond lengths range from 2.082-2.092 Å and bond indices span from 0.371-0.382). The Pt-N bonds of the complexes are, however, found to follow the reverse trend; the Pt–N_{10} bonds are stronger than the Pt–N_6 bonds. Concerning the data on the bond angle values, maximum deviations up to 3.7° and 4.8° (in aqueous phase) for the N_3–C_2–C_1 and C_4-C_5-N_6 angles respectively bear useful insights about the effects metal-coordination on the α-carbon geometries of the dipeptides. The geometries about the carboxylate C-atoms and the peptide linkages of the dipeptides too show largest variations up to 6.9° (C_2-C_1-O_7) and 2.2° (for both C_2-N_3-C_4 and N_3–C_4–C_5) respectively in the aqueous phase revealing the influence of complex formation on the intrinsic structural features of the dipeptides.

The gas and aqueous values of some structurally significant dihedral angles of the dipeptides and their metal complexes are listed in Table S4. Previous theoretical studies on dipeptides have revealed that the amide planes of small amino sequences are not completely planar, and therefore protein structure prediction based on a simplified model where only the Ramachandran dihedral angles (ψ

and ϕ) are taken into account is not adequate.[55] It is apparent from the values of the two dihedral angles viz. C_2-N_3-C_4-C_5 and H-N_3-C_4-O, considered to monitor the planarity of the peptide planes of the dipeptides and their complexes, that neither the non-ionic nor the dipolar zwitterionic form of the dipeptides possesses a completely planar amide plane. It is also interesting to note that metal coordination tends to disrupt the planarity of the peptide planes in the complexes. The predicted values of the ψ (N_3-C_4-C_5-N_6) and ϕ (C_1-C_2-N_3-C_4) dihedrals suggest that the backbone structural features of the dipeptides do not get modified dramatically in both gas and aqueous phases after metal coordination. On other hand, variations up to 39.8° in aqueous phase and 35.1° in gas phase in case of the N_3-C_2-C_1-O_8 dihedral can be attributed to geometry changes about the carboxylate groups of the dipeptides upon metal coordination.

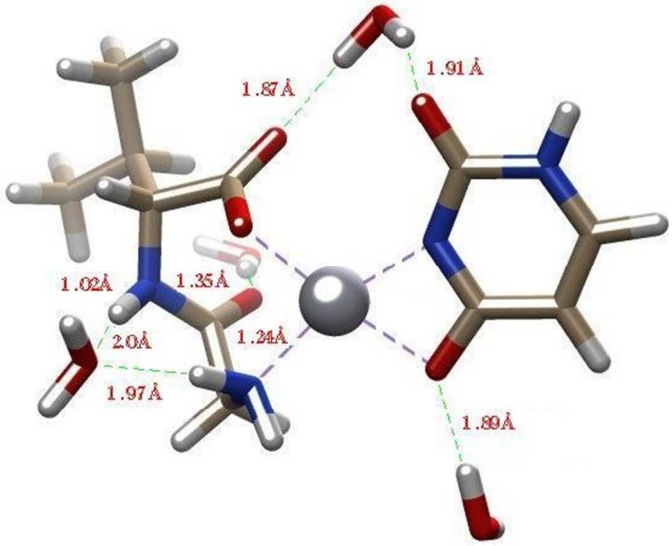

Fig. 5 Interactions of Pt(Ura)(GV) with explicit water molecules; denoted as ^{w}Pt(Ura)(GV)

Interactions of the water molecules with proteins *via* intermolecular H-bonds are crucial in order to afford the biologically active three-dimensional structures of proteins, and therefore the study of the interactions of water molecules with peptide moieties has been the subject matter of intense investigations.[43,56] The intermolecular H-bonds present in ^{w}Pt(Ura)(GV) are depicted in Fig. 5 along with their intermolecular H-bond distances. This figure also lists the bond length values of the N_3-H, C_4–N_3 and C_4=O bonds related to the amide plane geometry of the complex. As evident from the depiction, the interactions of the explicit water molecules with the amide planes of the Pt(Ura)(GV)

complex result in elongation of the exposed polar C_4=O and N_3–H bonds by a maximum value of 0.011 Å and shortening of the embedded N_3–C_4 bond up to 0.012 Å.

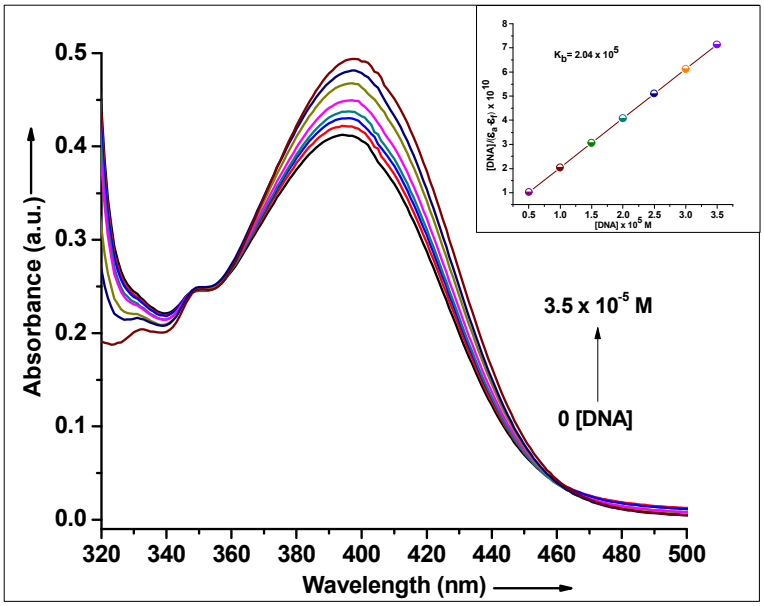

Fig. 6 Absorption spectra of the Pt(Ura)(GL) complex in the absence (black line) and presence of incremental amounts of CT-DNA (tris-buffer, pH 7); [Pt(Ura)(GL)]=10 μ*M*; [CT-DNA]=0-35 μ*M*; Inset: Linear plot shows the binding isotherms with CT-DNA.

DNA-binding properties. Low molecular weight metallopeptides are known to be efficient DNA binders, and have attracted much interest owing to their ability to serve as biomimetic models for metalloprotein-DNA interactions as well as for applications in biotechnology and medicine.[57,58] The absorption spectra of the Pt(Ura)(GL) complex at constant concentration (10 μM) in the absence and presence of different concentrations of CT-DNA (0-35 μM) are portrayed in Fig. 6. In the presence of increasing amounts of CT-DNA, the UV-vis titration spectra of the Pt(Ura)(GL) complex exhibit amplifications in the LMCT peak intensities at ~ 403 nm (hyperchromicity), while their absorption band-positions remain basically unaltered (i.e no batho- or hypsochromic shifts are observed). These results provide strong evidences regarding the possibilities of groove binding for the studied complex to DNA.[57,59] Groove-binding, mainly facilitated by the highly negative electrostatic potential of the DNA-grooves, has now been realized as an important non-covalent ligand-DNA binding motif in the field of drug development.[59] The K_b values for the interactions of the

Pt(Ura)(GL) complex with CT-DNA, calculated according to equation (I), is found to be 2.04 x 10^5 M^{-1}.

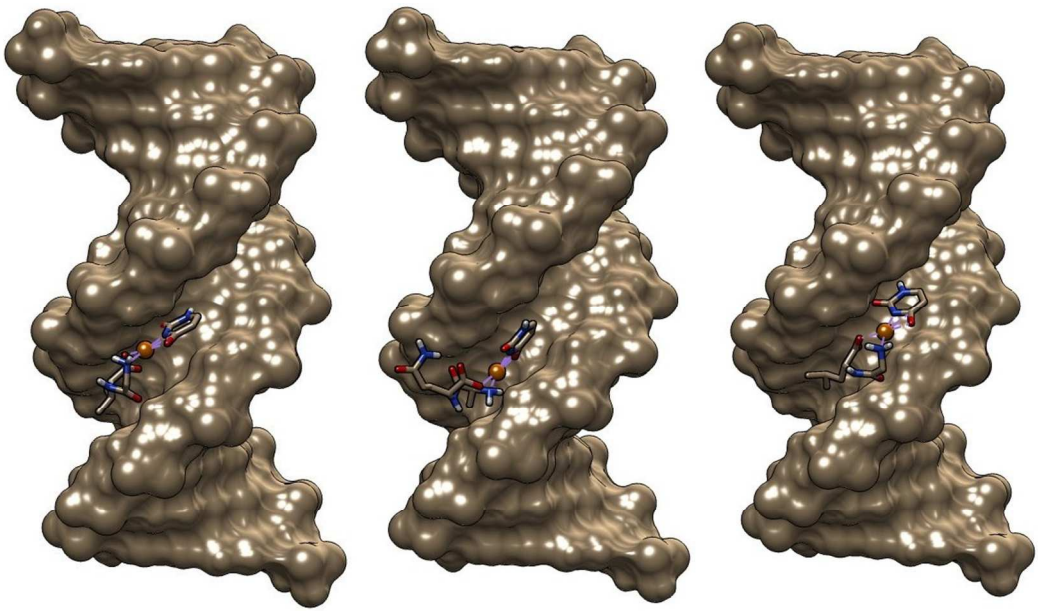

(a) Pt(Ura)(GV) (b) Pt(Ura)(AG) (c) Pt(Ura)(GL)

Fig. 7 Hydrogen bonded interactions of the studied systems with B-DNA

Docking procedures are now routinely used for *in silico* screening of the drug-receptor interactions because of their remarkable efficiency to describe the ‘‘best-fit’’ orientation of a ligand to a particular receptor; both energetically and geometrically. The efficacies and limitations of *in silico* studies as well as the current and future challenges in the realm of drug-receptor interaction chemistry have been recently reviewed.[60,61] It is known that the minor grooves of a double helical DNA molecule are the main binding sites for most of the antibiotic and anticancer drugs.[62,63] The highest ranking docked poses of the Pt(Ura)(GV), Pt(Ura)(AG) and Pt(Ura)(GL) complexes with the classical d(CGCGAATTCGCG)$_2$ B-DNA sequence are depicted in Fig 7. In general, the complexes are found to prefer the AT rich segment of the minor-groove of DNA. The H-bond interactions (whose intermolecular H-bond distances range from 1.51-2.06 Å) established by the complexes with DNA include the interactions of the O-atoms of the -CONH functions of the dipeptide moieties with the backbone -CH_2 groups and the C_2=O groups of uracil with the C_2-H groups belonging to the A6 residues of DNA. The predicted DNA binding-affinity order of the three complexes (Table S5), determined by performing single point energy calculations using the all atom potential UFF level, emerges as Pt(Ura)(AG) > Pt(Ura)(GL) > Pt(Ura)(GV).

Conclusions

The current work, aimed at studying the interactions of Pt(II) with uracil and small peptide moieties (i.e. glycyl-*l*-valine, glycyl-*l*-leucine and *l*-alanyl-*l*-glutamine) leading to the formation of peptide-nucleobase complexes, reveals that the dipeptides interact with the Pt(II) ion via their $–NH_2$ and $–CO_2^-$ groups in both solid and aqueous phases. Uracil binds to the metal ion through its N_3 and O_4 atoms. The non involvement of the dipeptide amide groups in metal binding is evidenced by the unchanged frequency values of the $\nu(N_3\text{-}H)$ and $\nu(C_4{=}O)$ modes in the dipeptides as well as in their metal complexes. Gas and aqueous phase theoretical calculations are carried out using the biologically relevant α_R conformers of the dipeptides at the B3LYP and B3PW91 levels in conjunction with the 6-31++G(d,p) and LANL2DZ basis sets in order to examine the influence of metal-coordination and solvation on the structural, electronic and vibrational properties of the complexes. Calculations show that the Pt(II)-peptide-nucleobase complexes exist in their low-spin states. Theoretically predicted square planar type geometries for the complexes are consistent with the experimentally observed absorption spectral data. Solvation effects of the continuum model as well as the explicitly considered aqueous phase are found to leave marked impression on the backbone structural aspects of the dipeptides. The vibrational modes of the ligands and their metallic complexes are better reproduced at B3LYP level as compared to those at B3PW91. UV-visible titration experiments in combination with *in silico* docking and molecular mechanical studies suggest that the metal complexes bind to the minor-groove of the DNA molecule, largely by H-bonding interactions.

Acknowledgments

Financial assistance from the Special Assistance Program of the University Grants Commission, New Delhi, India, to the Department of Chemistry, NEHU, is acknowledged. The analytical services provided by SAIF, NEHU are highly appreciated. S.M. is thankful to the University Grants Commission, New Delhi, India, for financial assistance through a research fellowship. The authors are grateful to Prof. R. H. Duncan Lyngdoh, NEHU, India, for providing computational facilities as well as to the reviewers for their probing and helpful comments.

References

1 M. Watabe, M. Kai, K. Goto, H. Ohmuro, S. Furukawa, N. Chikaraishi, T. Takayama and Y. Koike, *J. Inorg. Biochem.,* 2003, **97**, 240.

2 M. E. Dumont, J. W. Wiggins and S. B. Hayward, *Proc. Natl. Acad. Sci. USA,* 1981, **78,** 2947.

3 A. F. LeRoy, *Environ. Health Persp.,* 1975, **10**, 73.

4 F. J. Pesch, H. Preut and B. Lippert, *Inorganica. Chimica. Acta.,* 1990, **169**, 195.

5 R. B. Ciccarelli, M. J. Solomon, A. Varshavsky and S. J. Lippard, *Biochemistry*, 1985, **24**, 7533.

6 L. A. Moran, K. G. Scrimgeour, H. R. Horton, R. S. Ochs and J. D. Rawn, Biochemistry, 2nd ed. Prentice Hall: Englewood Cliffs, NJ, 1994.

7 R. Steininger, J. Karner, E. Roth and K. Langer, *Metabolism*, 1989, **38**, 78.

8 K. Tabata and S-I Hashimoto, *Appl. Environ. Microbial.*, 2007, **73**, 6378.

9 L. M. Gierasch and J. King, Eds. Protein Folding, Deciphering the Second Half of the Genetic Code; American Association for the Advancement of Science: Washington, DC, 1990.

10 P. D. Bailey, An Introduction to Peptide Chemistry; John Wiley and Sons: New York, 1992.

11 Y. Jin and J. A. Cowan, *J. Am. Chem. Soc.*, 2006, **128**, 410.

12 Z. Martins, O. Botta, M. L. Fogel, M. A. Sephton, D. P. Glavin, J. S. Watson, J. P. Jason P. Dworkin, A. W. Schwartz, P. Ehrenfreund, *Earth Planet. Sci. Lett,.* 2008, **270**, 130.

13 B. Lippert, *Inorg. Chem.,* 1981, **20**, 4326.

14 M. Goodgame and K.W. Johns, *J. Chem. Soc., Dalton Trans.*, 1977, **17**, 1680.

15 M. S. Masoud, A. A. Ibrahim, E. A. Khalil and A. El-Marghany, *Spectrochimica. Acta. Part A* 2007, **67**, 662.

16 S. A. Krasnokutski, J. S. Lee and D-S. Yang, *J. Chem. Phys.,* 2010, **132**, 044304/1.

17 E. A. L. Gillis, K. Rajabi and T. D. Fridgen, *J. Phys. Chem. A,* 2009, **113***,* 824.

18 H. Tavakol, *Arabian Journal of Chemistry*, Article in press, 2013, http://dx.doi.org/10.1016/j.arabjc.2012.12.007

19 S. Mandal, G. Das and H. Askari, *Struct. Chem.,* 2014, **25**, 43.

20 M. E. Reichmann, S. A. Rice, C. A. Thomos and P. Dohi, *J. Am. Chem. Soc*., 1954, **76**, 3047.

21 C. V. Kumar and E. H. Asuncion, *J. Am. Chem. Soc.,* 1993, **115**, 8547.

22 A. D. Becke, *J. Chem. Phys.* 1993, **98**, 5648.

23 C. Lee, W. Yang and R. G. Parr, *Phys. Rev. B,* 1988, **37**, 785.

24 J. P. Perdew and Y. Wang, *Phys. Rev. B*, 1992, **45**, 13244.

25 A. J. H. Wachters, Gaussian *J. Chem. Phys.,* 1970, **52**, 1033.

26 P. J. Hay, *J. Chem. Phys.* 1977, **66**, 4377.

27 W. R. Wadt and P. J. Hay, *J. Chem. Phys.,* 1985, **82**, 284.

28 P. J. Hay and W. R. Wadt, *J. Chem. Phys.* 1985, **82**, 299.

29 M. J. Frisch, G. W. Trucks, H. B. Schlegel, G. E. Scuseria, M. A. Robb, J. R. Cheeseman, G. Scalmani, V. Barone, B. Mennucci, G. A. Petersson, H. Nakatsuji, M. Caricato, X. Li, H. P. Hratchian, A. F. Izmaylov, J. Bloino, G. Zheng, J. L. Sonnenberg, M. Hada, M. Ehara, K. Toyota, R. Fukuda, J. Hasegawa, M. Ishida, T. Nakajima, Y. Honda, O. Kitao, H. Nakai, T. Vreven, J. A. Montgomery Jr., J. E. Peralta, F. Ogliaro, M. Bearpark, J. J. Heyd, E. Brothers, K. N. Kudin, V. N. Staroverov, T. Keith, R. Kobayashi, J. Normand, K. Raghavachari, A. Rendell, J. C. Burant, S. S. Iyengar, J. Tomasi, M. Cossi, N. Rega, J. M. Millam, M. Klene, J. E. Knox, J. B. Cross, V. Bakken, C. Adamo, J. Jaramillo, R. Gomperts, R. E. Stratmann, O. Yazyev, A. J. Austin, R. Cammi, C. Pomelli, J. W. Ochterski, R. L. Martin, K. Morokuma, V. G. Zakrzewski, G. A. Voth, P. Salvador, J. J. Dannenberg, S. Dapprich, A. D. Daniels, O. Farkas, J. B. Foresman, J. V. Ortiz, J. Cioslowski and D. J. Fox, Gaussian 09, revision C.01; Gaussian, Inc.: Wallingford, CT, 2010.

30 S. Miertus, E. Scrocco and J. Tomasi, *Chem. Phys.,* 1981, **55,** 117.

31 M. Marin-Luna, G. Sanchez-Sanz, P. O'Sullivan and I. Rozas, *J. Phys. Chem. A,* 2014, **118**, 5540.

32 N. Takagi and S. Sakaki, *J. Am. Chem. Soc.,* 2012, **134**, 11749.

33 S. Mandal, G. Das and H. Askari, *J. Chem. Inf. Model.,* 2014, **54**, 2524.

34 I. R. Gould, W. D. Cornell and I. H. Hillier, *J. Am. Chem. Soc.,* 1994, **116**, 9250..

35 J. B. Foresman and A. Frisch, Exploring Chemistry with Electronic Structure Methods, 2nd ed.; Gaussian, Inc.: Pittsburgh, PA, 1996.

36 R. Bauernschmitt and R. Ahlrichs, *Chem. Phys. Lett.,* 1996, **256**, 454.

37 D. W. Ritche and V. Venkataraman, *Bioinformatics*, 2010, **26**, 2398.

38 M. D. Hanwell, D. E. Curtis, D. C. Lonie, T. Vandermeersch, E. Zurek and G. R. Hutchison, *J Cheminform.,* 2012, **4**, 1.

39 E. F. Pettersen, T. D. Goddard, C. C. Huang, G. S. Couch, D. M. Greenblatt, E. C. Meng and T. E. Ferrin, *J. Comput. Chem.*, 2004, **25**, 1605.

40 G. N. Ramachandran, *Biopolymers,* 1963, **6**, 1494.

41 G. N. Ramachandran, C. Ramakrishnan and V. Sasisekharan, *J. Mol. Biol.,* 1963, *7*, 95.

42 Z. X. Wang and Y. Duan, *J. Comp. Chem.,* 2004, **25**, 1699.

43 S. Mandal, R. H. D. Lyngdoh, H. Askari, and G. Das, *J. Chem. Eng. Data*, 2015, **60**, 659.

44 J. Ni, Y-G. Wang, H-H. Wang, L. Xu, Y-Q. Zhao, Y-Z. Pan and J-J Zhang, *Dalton Trans.*, 2014, **43**, 352.

45 K. Fukui, T. Yonezawa and H. Shingu, *J. Chem. Phys.* ,**1**952, **20**, 722.

46 J. T. L. Navarrete, V. Hernandez and F. J. Ramirez, *J. Mol. Struct.,* 1995, **348**, 249.

47 K. Nakamoto, Y. Morimoto and A. E. Martell, *J. Am. Chem. Soc.,* 1961, **83**, 4528.

48 A. W. Herlinger, S. L. Wenhold and T. V. Long, *J. Am. Chem. Soc.,* 1970, **92,** 6474.

49 P. R. Reddy, N. Raju and K. V. Reddy, *Indian J. Chem.,* 2009, **48A**, 1638.

50 I. R. Gould, M. A. Vincent and I. H. Hillier, *J. Chem. Soc. Perkin Trans.,* 1992, **2**, 69.

51 A.R. Sarkar and P. Ghosh, *Inorganica Chimica Acta,* 1983, **78**, L39.

52 W. J. Hehre, L. Radom, P. v. R. Schleyer and J. A. Pople, Ab initio molecular orbital theory. Wiley, New York, 1986.

53 F. D. Proft, J. M. L. Martin, P. Geerlings, *Chem. Phys. Lett.,* 1996, **250**, 393.

54 K. B. Wiberg, *Tetrahedron,* 1968, **24**, 1083.

55 C. D. Keefe and J. K. Pearson, *J. Mol. Struct. (Theochem.),* 2004, **679**, 65.

56 N. A. Besley and J. D. Hirst, *J. Am. Chem. Soc.,* 1999, **121**, 8559.

57 S. Parveen, F. Arjmand and D. K. Mohapatra, *J. Photochem. Photobiol. B, Biol.,* 2013, **126**, 78.

58 N. Y. Sardesai, K. Zimmermann and J. K. Barton, *J. Am. Chem. Soc.,* 1994, **116**, 7502.

59 G. Barone, A. Terenzi, A. Lauria, A. M. Almerico, J. M. Leal, N. Busto and B. Garcia, *Coord. Chem. Rev.,* 2013, **257**, 2848.

60 A. V. Vargiu and A. Magistrato, *Chem. Med. Chem.*, 2014, **9**, 1966

61 K. Spiegel and A. Magistrato, *Org. Biomol. Chem.*, 2006, **4**, 2507

62 S. Neidle, *Nat. Prod. Rep*., 2001, **18**, 291.

63 X. Gao, P. Mirau and D. J. Patel, *J. Mol. Biol.,* 1992, **223**, 259.